PART I: Extended summary

I.1 Introduction: scope, objectives and the audience of guidelines

I.1.1 Motivation

Aqueous-solid solution (Aq-SS) systems are ubiquitous both in natural and anthropogenic environments. In most nuclear waste repositories, solid solutions are intrinsic constituents of the various components of the repository system: from the waste source to the geosphere/biosphere interface.

Many components in UO_2 and MOX spent nuclear fuel are present as solid solutions of the UO_2 matrix, and their dissolution behaviour can be explained in the framework of Aq-SS, as we will illustrate in a later example in Chapter II.3. A similar situation has been described for the behaviour of trace components in the altered layer of vitrified nuclear wastes [2001GRA/MUL]. Cement, which is a central component in many designs and an unavoidable one in others, builds through its alteration an array of calcium silicate hydrate solid solution phases, commonly known as CSH. The corrosion of steel containers and cast iron inlets produces a variety of Fe(III)/Fe(II) oxyhydroxide solid phases which are able to incorporate trace components in their structures. While initially the trace metal interactions are mainly controlled by adsorption processes and described by surface complexation models [1990DZO/MOR] the evolution of these Fe(III) oxyhydroxide phases with time (ageing) and their interactions with contacting fluids may be described also in the context of Aq-SS systems. We will discuss in Section I.4 the evolution pathway of the various sorption processes and their influence upon the fate of trace metals in aqueous-solid systems.

Bentonite, which is one of the preferred backfill components in repository systems, contains both carbonates and sulphates as accessory minerals. The interaction of groundwater with the bentonite material produces the dissolution and reprecipitation of these carbonates and sulphates, mainly as calcite and gypsum. The behaviour of trace metals in these systems can be also modelled as an Aq-SS system. Besides, clay miner-

als montmorillonite and illite can also be treated as solid solutions, both with respect to cationic substitutions in the T-O-T layer and on particle edges, and regarding interlayer cation exchange.

The dissolution and precipitation of carbonates, sulphates and Fe(II)/Fe(III) oxyhidroxides is an ongoing process in many clay and granitic geosphere environments. Again, the solubility behaviour of the trace radionuclides in these environments cannot be decoupled from these main systems and their solubility behaviour is better approached by using the Aq-SS concept.

The thermodynamics of solid solutions/aqueous solutions are commonly used in metallurgy, ceramics and mineralogy, although the applicability of the concepts and methodologies to low temperature aqueous geochemical systems has been more limited. This is mainly due to the fact that solid diffusion is expected to be slow at low temperatures. However, as we will discuss later on, many solid phases show a remarkable structural flexibility to incorporate trace components even in situations when ionic size and charge are not the most favourable.

In this document, the specific emphasis is put on Aq-SS systems where partitioning of chemical elements of interest occurs between the solid solution and the aqueous electrolyte phases. Such systems are more complex than simpler systems involving solubility of stoichiometric solids or ion exchange. Only recently (since the 1980s), rigorous theoretical approaches have become available for Aq-SS systems (see Section II.1.2). All known features of Aq-SS behaviour show their fundamental property: the "dilution" of a minority (possibly hazardous) element in the host solid solution can greatly decrease its dissolved aqueous concentrations and, hence, mobility, compared with the case when the minority (hazardous) element forms its own "pure" solid phase. But it can also accumulate, for example, radionuclides beyond their assumed adsorption concentrations. This kind of radionuclide accumulation is then much more difficult to be mobilised when the geochemical conditions change.

Presently, the geochemical models used in the various stages of the safety assessment of a nuclear waste repository do not incorporate solid solutions in an explicit manner in the treatment of the solubility (and subsequent migration) of trace radionuclides, neither in the near nor in the far field of the repository system. While the solid solution concept is implicitly incorporated in the partition/distribution coefficients used to describe the overall radionuclide sorption process, only in the case of the solubility of Ra(II), the formation of Ra(II)/Ba(II) sulphate solid solutions has been taken into consideration [1999SKB]. The fact that solid solution formation is not considered as an acting process for radionuclide retardation has been justified in the grounds of a pessimistic consideration of the retardation capacity of the near field and the geosphere. But as already pointed out by Glynn [2003GLY], the formation of solid solutions may lead to radionuclide accumulation in certain parts of the system. These accumulations may

be later released when the geochemical conditions (redox, alkalinity…) change. In [2003GLY] this was exemplified by the oscillatory behaviour of Np and Pu pulses.

Except in some particular cases and certainly not in a systematic way, the thermodynamic properties of solid solutions have been also explicitly avoided in the previous review exercises performed within the various phases of the NEA TDB project ([1992GRE/FUG], [1995SIL/BID], [1999RAR/RAN], [2001LEM/FUG], [2003GUI/FAN], [2005OLI/NOL], [2005GAM/BUG], [2005BRO/CUR], [2005HUM/AND]). This was mainly due to the lack of agreed Guidelines concerning their treatment.

The Management Board of the OECD NEA TDB III Project felt in initiating an activity in the Programme of work of the Project leading to the preparation of scientific guidelines to assist in the evaluation and application of solid solution and Aq-SS systems in thermodynamic models.

I.1.2 Objectives

Hence, the objectives of this document are:

- To present state-of-the-art theoretical concepts and methods of solid solution thermodynamics from different scientific fields in order to propose methods to interpret and model experimental data for Aq-SS systems.
- To identify potential theoretical and experimental gaps that hinder the full applicability of Aq-SS systems in waste management.
- To provide guidance for the compilation and interpretation of solid solution thermodynamic data, both for experimenters and for reviewers within the NEA TDB Project.
- To present criteria and methods to model relevant Aq-SS systems.
- To present case studies which show the application of solid solution thermodynamics and Aq-SS systems in nuclear waste management-relevant uses and their potential application to the Performance Assessment of nuclear waste repositories.

I.1.3 Audience

The Guidelines contained in this document are in the first place directed to the various present and future expert review teams within the NEA TDB project in order to help them to use, interpret and incorporate aqueous-solid solution systems in their review work. In addition the Guidelines intend to target potential experimental groups in order to assist them to design experiments and interpret their solid solution experimental data in a way suitable to be incorporated in the current TDB efforts. The final outcome of these Guidelines should also be helpful to performance assessment modellers in order to stimulate them to incorporate such a relevant and ubiquitous concept for radionuclide

retention and, in turn, to provide a more scientifically robust description of the radionuclide migration in the various components of a repository system.

I.1.4 Scope

Since these Guidelines are mainly directed to the application of thermodynamic aqueous-solid solution models in the Performance Assessment of nuclear waste repositories, the emphasis will be placed on the solubility behaviour of radionuclide trace components incorporated into relevant host minerals (oxyhydroxides, carbonates, sulphates, sulphides, phosphates, clays) and anthropogenic materials (UO_2 solid solution and cements).

We limit our discussion to low temperature (t < 100 ºC) and atmospheric pressure systems and methods for temperature and pressure corrections (important for solid solutions considered in petrology and metallurgy) are largely left behind the scenes. This would in principle entail a number of kinetic restrictions to the solid solution formation process. However, consideration has to be given to phenomena such as the long residence times of water in the various parts of the repository system, the increased lithostatic and hydrostatic pressures in the geosphere and to the fact that, as we will document later in Section I.3, there is strong evidence of solid solution formation at low temperatures, particularly in soil systems where this process has been studied from the molecular point of view. However, specific methods of temperature and pressure corrections of thermodynamic properties (important for solid solutions considered in petrology and metallurgy) are largely left behind the scenes.

The elements to be considered will include those radionuclides for which there is fundamental evidence that their solubility behaviour is better rationalised in terms of Aq-SS systems. These are mainly actinides (U, Am, Cm), lanthanides (Eu) and some alkaline earth (Sr, Ra) and even more importantly some anionic fission products like selenate, and selenide that are known to substitute sulphate and sulphide in many mineral phases.

I.2 Definitions

These basic notions and definitions (mostly corresponding to IUPAC recommendations) are used and elaborated throughout the Guidelines. They are collected here to avoid misunderstandings or misinterpretations. Additional definitions will be provided in Section I.3 when describing the evolution between aqueous and solid solutions.

Phase is a homogeneous part of the (chemical) system such that temperature, pressure, and concentrations of the components are uniform within it. Different phases are separated by physical boundaries and can exist in solid, liquid, or gaseous aggregate states.

A **Mechanical mixture** can be viewed as a composition of two or more phases that are not chemically combined with each other and can be separated by mechanical means.

Miscibility is the ability of two or more substances to mix and form a single homogeneous phase called "solution".

Aqueous solution is a homogeneous mixture of one or more substances (the solutes) dissolved in another substance (the solvent - water). For example, a salt and a gas dissolved in water.

Solid solution is a homogeneous crystalline structure in which one or more types of atoms or molecules may be partly substituted for the original atoms and molecules without changing the structure, although the lattice parameters may vary.

Thermodynamically, the **composition** of a solid solution or an aqueous solution is expressed through concentrations of one or more chemical species (substances, components, end-members).

Composition of a **pure** (stoichiometric) **phase** can be described using one substance only, *i.e.*, it can appear in any system only having a definite constant (elemental) **stoichiometry** unequivocally related to structure. Examples are simple minerals like quartz SiO_2 or portlandite $Ca(OH)_2$.

Composition of a **solution** (multicomponent) **phase** needs two or more end-members for describing the whole range of it. Each **end-member** (species) must have a fixed elemental stoichiometry, but may have a variable concentration (*e.g.*, **mole fraction**) in the solution phase whose structure remains intact (with some minor change). Hence, the bulk elemental composition of a solution phase is variable. For example, the solid solution of Fe and Mn carbonate $(Fe,Mn)CO_3$ can be described as a homogeneous mixture $(1–x)FeCO_3 + xMnCO_3$ of two end-members $FeCO_3$ and $MnCO_3$ where x is the mole fraction of $MnCO_3$. In equilibrium with other phases present in the system, this mole fraction can take values from 0 (pure $FeCO_3$) to 1 (pure $MnCO_3$) depending on temperature, pressure and bulk elemental composition of the whole system.

Thermodynamically, an **ideal solution** is a solution where the enthalpy (heat) of solution is zero (see Section II.1.1). Any other solution is called **non-ideal**. The simplest regular non-ideal mixing model ignores non-configurational contributions to the entropy of mixing, assuming a zero excess entropy of mixing as a good first approximation.

In equilibrium between an ideal solution phase and an ideal gas, the partial (vapor) pressures of solution end-members are proportional to their mole fractions (**Raoult's law**). For simple ideal solid solutions, this law is often formulated in a different way: activities of end-members are equal to their mole fractions.

In real (solid) solutions, the thermodynamic **activities** of end-members differ from their mole fractions. To correct for that, the *activity coefficients* f_j defined through $a_j = f_j\, x_j$ are used (more in Chapter II.1). **Activity coefficients** are (often complicated) functions of the solution phase composition, usually defined such that the activity coef-

ficient of end-member equals 1 at its mole fraction $x = 1$ and approaches a constant at $x \to 0$. Various expressions for activity coefficients of solid solution end-members derived from the **excess** Gibbs energy of mixing G_m^E as function of phase composition, are considered in Section II.1.2.1.

Depending on the reference state convention used for the *j*-th component, the activity coefficient is denoted f_j (*symmetrical* convention used for gases, solid end-members and water solvent) or γ_j (*unsymmetrical* convention, used for solutes in aqueous electrolyte and solutes in dilute solid solutions). In literature, activity coefficients for solid end-members were sometimes denoted λ_j, which is not recommended by IUPAC and NEA TDB (f_j should be used instead).

The behaviour of a "trace" end-member ($x < 0.01$) is well approximated by **Henry's law**, originally stating that the mass of a gas dissolved in a definite volume of liquid is directly proportional to the partial pressure of the gas. This law is applicable to **dilute** components of all kinds of solutions (solid, aqueous, surface *etc*.). The coefficient of proportionality is called the Henry constant, k_H , and is related to a value of activity coefficient at infinite dilution.

Partition of a component (element) between two solution phases is usually characterised by a **distribution ratio** R_d (distribution coefficient) – a ratio of concentration of this component in one phase to that in another phase. This empirical value applies both to equilibrium and non-equilibrium situations. In the case of equilibrium, a ratio of concentrations of the same component M in two phases is called the **distribution constant** k_D. At low concentrations (*e.g*., for trace components), this constant defines the position of a (linear) uptake **isotherm** - a plot of concentration of M in solid solution *vs.* dissolved aqueous concentration of M.

Sometimes, for (B,C)L solutions, the **distribution coefficient** *D* is defined as the ratio of x_B/x_C (mole fractions of BL and CL) to $m_{B,aq}/m_{C,aq}$ (molalities of B and C, see Section II.1.2.1).

Solubility equilibrium in a strict sense describes the chemical equilibrium between the pure (solid) and the dissolved states of a compound. In the context of these Guidelines, "dissolved" is usually understood as dissolved in aqueous electrolyte. In the simplest case (*e.g*., dissolution of quartz at neutral pH), this is described by a reaction B(solid) $\rightleftharpoons$ B(aqueous) with **equilibrium constant** K_s . An ionic solid like ML dissolves to aqueous cations M^+ and anions L^- (or M^{2+}, L^{2-}, …), ML = $M^+ + L^-$. An equilibrium constant of such reaction is called the solubility product, $K_{s,0} = \{M^+\}\{L^-\}$ (braces denote ion activities). Other cases are described in Section II.1.2.1.

In a more general case (including equilibrium and non-equilibrium), the ion activity product $\{M^+\}\{L^-\}$ can be divided by the solubility product $K_{s,0}$ to obtain a **saturation index** SI. The case SI = 1 corresponds to equilibrium (saturation). If SI < 1 then

the aqueous solution is undersaturated to ML solid; if SI > 1, the aqueous phase is oversaturated.

Simple solubility relationships for a pure solid become more complex if the solid solution (*i.e.*, variable-composition solid) is dissolved. Such dependencies are usually represented using solubility products of pure end-members, *e.g.*, $K_{SP,BL}$, $K_{SP,CL}$, keeping in mind that their activities are no longer unity. There are two approaches – the **Lippmann functions** and diagrams, and the **unified theory** of solid solution solubility by Gamsjäger and Königsberger, both described in detail in Sections II.1.2.1 and II.1.2.2.

Theoretical approaches operate mainly with activities of dissolved components, while in experiments, the aqueous concentrations (molalities, molarities) are determined, often at high background electrolyte concentration (ionic strength). At such conditions, the activity of aqueous ion may be several times different from its measured concentration. This difference is accounted for by **aqueous activity coefficients** (see Section II.1.2.1) which must be considered in interpretation of almost any solubility data.

Further specific definitions about the various equilibrium status in Aq-SS systems, equilibrium, primary saturation, stoichiometric saturation and so on, are given in the following sections, where the theoretical grounds (fully developed in Part II, Section II.1) and the experimental techniques (detailed in Part II, Section II.2) are introduced.

I.3 From Aqueous to Solid Solutions

This section intends to demonstrate that there is a continuum between the processes that control the fate of trace components in the aqueous and solid phases.

From the process perspective we may describe the transfer and partitioning of chemical components between an aqueous phase and an adjacent solid phase under the general term of **Sorption.**

Mechanistically, sorption may occur through different mechanisms but the main ones from the perspective of this work are listed below.

Adsorption: the accumulation of the chemical component at the interface between the aqueous phase and an already existing solid phase without the development of a three-dimensional molecular arrangement. This is presently rationalised from a mechanistic point of view by using surface complexation models which integrate in the thermodynamic framework the electrostatic interactions and the chemical bonding between the adsorbed chemical species and the solid surface.

Absorption: the uptake through the diffusion of an (aqueous) chemical component into the whole volume of the existing (micro/nanoporous) solid phase (*e.g.*, in zeolites).

Precipitation: the transfer of an aqueous chemical component into the solid phase by growing a three dimensional molecular arrangement – the crystal structure. Precipitation may be initiated by a *homogeneous nucleation* forming a pure solid phase, or by a *heterogeneous nucleation* and growth into an already existing solid phase by inclusion or by precipitation onto an existing surface; the latter is known as **surface precipitation**.

Co-precipitation: the precipitation and crystal growth process, in which the minor component of interest forms a common (mixed-composition) structure with the major (host) component. This requires a certain oversaturation of aqueous solution with respect to pure major component, while most often an undersaturation with the pure minor component.

Recrystallisation: the process of rebuilding the crystal structure of the host solid solution in contact with the aqueous phase into the same type of structure, but possibly with different concentrations of minor components as a response to changes in composition, temperature and pressure in the system.

As previously defined a **solid solution** is a homogeneous crystalline structure in which one or more types of atoms or molecules may be partly substituted for the original atoms and molecules without changing the structure, although the lattice parameters may vary. The solid components are regularly ordered in a periodic three dimensional structure.

Adsorption, co-precipitation and surface precipitation are precursory mechanisms for the formation of solid solutions, although the regular molecular arrangement in a three dimensional structure requires additional processes like ion-diffusion into the solid and recrystallisation of the initial solid phase.

In the time scale, adsorption normally precedes the formation of surface precipitates and, therefore, there is certain continuity in the following process chain (arranged from short to long reaction times):

Aqueous complexation ⇒ Adsorption (surface complexation) ⇒ Absorption ⇒ Surface precipitation ⇒ Co-precipitation ⇒ Ion-diffusion ⇒ Solid Solution recrystallisation.

Figure I-1, extracted from Manceau *et al*. [2002MAN/MAR], gives an indication of the complexity and richness of the various sorption processes (governing the element partition between solid and aqueous phases) involved in natural systems.

Sorption is a key process in the retardation of radionuclides in the geosphere. As we can see, it involves a number of processes which are substantially different from the molecular point of view and occur in different time scales. A fundamental finding which is easily forgotten is that molecular processes have to be investigated at the molecular level. The macroscopic approximation (mass balance studies), although neces-

sary, it is never sufficient to distinguish between the various sorption processes, this was already pointed out by Sposito [1986SPO]. In addition, the incorrect identification of the sorption processes may lead to an inaccurate quantification of the process and consequently in their application to Performance Assessment as it has recently been illustrated by Glynn [2003GLY].

Figure I-1: Basic processes of absorbate molecules or atoms at mineral-water interface. a) physisorption; b) chemisorption; c) detachment; d) absorption or inclusion; e) occlusion; f) attachment; g) hetero-nucleation; h) organo-mineral complexation; i) complexation to bacterial exopolymer and to cell outer membrane (extracted from Manceau *et al*. [2002MAN/MAR]). Reprinted from [2002MAN/MAR], Copyright (2002), with permission from the Mineralogical Society of America.

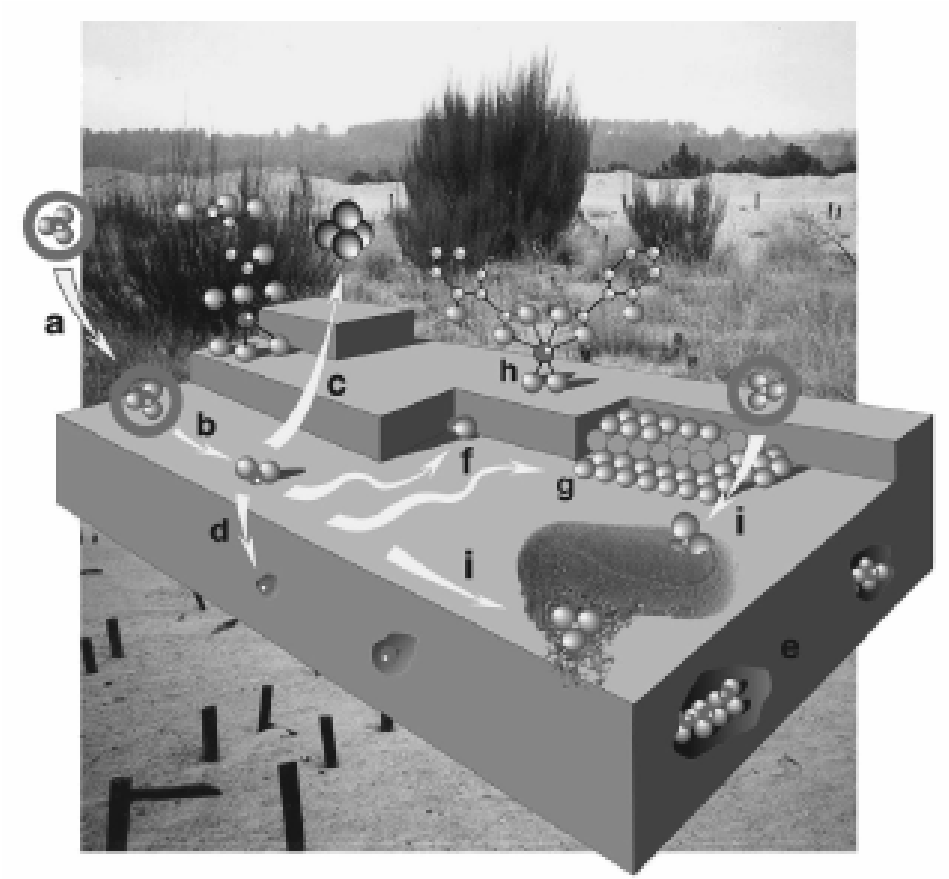

As we will discuss in Section II.2, the development and application of molecular and atomic spectroscopic techniques is key to the understanding and quantification of the Aqueous-Solid Solution processes and a prerequisite to their thermodynamic description.

It is interesting to point out in this context, that several spectroscopic techniques have been applied for discerning the various sorption processes as described in Part II, Chapter II.2, since the pioneering work of McBride in the use of Electron Spin Resonance (ESR) for discriminating the bonding environment of Mn^{2+} in carbonate phases [1982MCB]. The combination of ESR and solution chemical studies was used by Wersin *et al*. [1989WER/CHA] to describe the continuous transition between Mn^{2+} sorption and surface precipitation on siderite ($FeCO_3$(s)), as a function of the siderite surface coverage by Mn^{2+} The same process continuity has been found to describe the sorption products of Pb(II) onto the calcite surface investigated by Rouff *et al*. [2004ROU/ELZ] by a combination of batch tests and X-Ray absorption spectroscopy. Depending on the calcite surface coverage by Pb(II) the sorption mechanism changes from mononuclear inner sphere surface complexation to the surface precipitation of cerussite and hydrocerussite phases. The sorption continuity process is not only constrained to carbonates. The application of EXAFS spectroscopy and chemical solution methods to the investigation of the sorption of Zn(II) onto alumina oxides indicated the transition from Zn^{2+} bidentate complexes onto the alumina surface to the formation of Zn-hydrotalcite like nanophases as precursors of their co-precipitation [2000TRA/BRO].

A common thread in all these studies is that the transition between adsorption (surface complexation) and the formation of distinct trace component solid phases as surface precipitates occurs at trace metal surface coverage in the range 10^{-6} to 10^{-5} mol·m^{-2}.

The transition from the adsorbed layer or surface precipitate to solid solution is more difficult to ascertain, particularly at ambient temperatures, where ion diffusitivities in the solid phases are low, and where the recrystallisation and the epitaxial growth appear to be the only plausible mechanisms for the formation of solid solutions at low temperature.

There are some examples of low temperature solid solution formation *via* diffusion and recrystallisation, mainly for divalent carbonates. This is based on the fact that the diffusion coefficient of divalent cations in calcite is of the order of magnitude of 10^{-19} to 10^{-20} cm^2·s^{-1} [1964LAH/BOL], which gives depths of penetration of some 3 nm in two weeks [1992STI/HOC]. These authors presented a convincing case for the formation of $CdCO_3$/$CaCO_3$ solid solution formation through surface complexation of Cd^{2+} on the $CaCO_3$ surface followed by Cd^{2+} diffusion into the calcite lattice at ambient temperature. Similar mechanisms have been proposed to operate for other divalent cation calcium carbonate solid solution formation at low temperature. Low temperature diffu-

sion of cations into solid lattices is not only restricted to carbonates. In the soil science literature there are numerous examples of cation diffusion into Fe(III) oxyhydroxides, see for instance [1988BRU/GER] where they report evidence of the diffusion of Ni^{2+}, Zn^{2+} and Cd^{2+} into goethite.

While ferrites have been reported to be high temperature phases, Pérez-Perales and Umetsu [2002PER/UME] have investigated the formation of Zn(II) ferrites by a combination of solution chemistry diffraction and spectroscopic (XRD, EMPA, SEM) techniques. Their work indicates that crystalline Zn-ferrites are formed at low temperatures (25 ºC) when the appropriated redox, acidity and Zn/Fe ratios are satisfied.

Epitaxial growth and recrystallisation has been reported as solid solution formation mechanism for a number of aluminosilicate phases. The development of EXAFS spectroscopic techniques has been very useful in order to establish this mechanism for the solid solution formation at low temperature. As an example, we include in Figure I-2 the formation sequence of Zn/Mg phyllosilicate as monitored by EXAFS [2002MAN/MAR].

Figure I-2: Formation sequence of Zn/Mg phyllosilicate as monitored by EXAFS. Reprinted from [2002MAN/MAR], Copyright (2002), with permission from the Mineralogical Society of America.

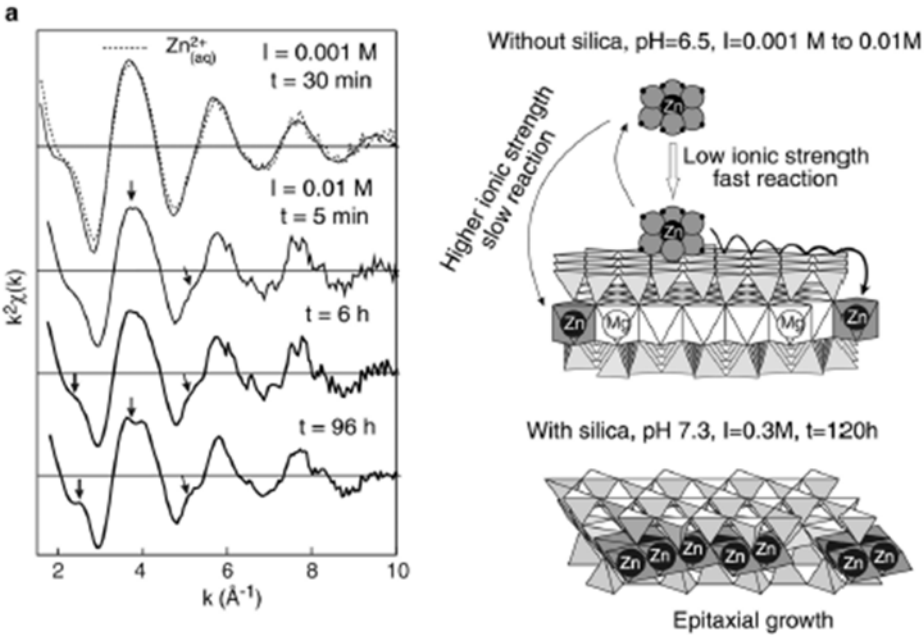

Another example of low temperature (5 - 15 ºC) rapid solution formation is encountered in the various phase transformations resulting from the sulphate attack on cement. Köhler *et al*. [2006KOH/HEI] report the effect of ettringite on thaumasite formation by studying pastes mixed using synthetic clinker phases, fly ash and nanosilica. The results indicate that thaumasite formation occurs through the heterogeneous nucleation of thaumasite on the surface of ettringite, due to the structural similarities of these minerals. This reaction is followed by further epitaxial growth of thaumasite from its components present in solution. Similar observations have been made by Blanco-Varela *et al*. [2003BLA/AGU].

It should be clear from the previous discussion that the transition of a trace component from being an aqueous solute to finally become a solid solute entails a number of complex processes which may occur sequentially and also in parallel. The thermodynamic description of the Aq-SS processes has to some extent acknowledged this complexity. Macroscopic determinations have to be complemented by proper molecular level spectroscopic analyses in order to gain the process understanding. This is further stressed in the discussion of the experimental methodologies for the determination of Aq-SS equilibria in Part II, Chapter II.2.

I.4 Basic thermodynamics of Solid Solutions

This section intends to bring into this Part I the basic concepts related to the thermodynamic description of Aqueous Solution-Solid Solution systems. A more detailed account is given in Part II, Chapter II.1 of this document.

Consider the general reaction:

$$x_A A(s) + x_B B(s) \rightleftharpoons A(x_A)B(x_B)(s) \qquad (I.1)$$

where A(s) and B(s) are the end-members which mix to form a homogeneous solid solution of intermediate composition described with mole fractions, x_A, x_B (in a binary system, $x_A + x_B = 1$).

At atmospheric pressure and temperature T, the Gibbs energy per mole of an isostructural binary solid solution can be written as:

$$\Delta G_m \text{ (solid solution, } T) = x_A\, G^o_m(A, T) + x_B\, G^o_m(B, T) + \Delta G_m \text{ (mix)} \qquad (I.2)$$

where ΔG_m (solid solution, T) is the standard Gibbs energy of the solid solution, G^o_m(A, T) and G^o_m(B, T) are the standard Gibbs energies of the end-members A and B, and ΔG_m (mix) is a Gibbs energy of mixing term. Note that throughout this section, the superscript zero refers to the standard state of pure component, $x = 1$.

The ΔG_m (mix) term consists of an enthalpy and entropy terms:

$$\Delta G_m \text{ (mix)} = \Delta H_m \text{ (mix)} - T\Delta S_m \text{ (mix)} \qquad (I.3)$$

The conceptualisation and quantification of the Gibbs energy of mixing is a fundamental issue in the determination and application of Aq-SS thermodynamics and it will be tackled in Parts 1 and 2 of this work both from the theoretical, the experimental and the modelling perspectives. In the following sections we will briefly discuss the nature of the contributors to the Gibbs energy of mixing in solid solution systems, this is the enthalpy and entropy of mixing. A more thorough discussion is found in Chapter II.1 of Part II.

I.4.1 The enthalpy of mixing

The enthalpy of mixing term contains the energetics of the interactions. Positive $\Delta H_{\mathrm{m}}^{\mathrm{o}}$ (mix) generally indicates clustering of like species and a tendency toward exsolution, while a negative $\Delta H_{\mathrm{m}}^{\mathrm{o}}$ (mix), generally suggests ordering of unlike species and a tendency toward formation of an intermediate compound. Both tendencies may occur simultaneously in the same system (see the examples of carbonates and feldspars in Chapter II.1 of Part II).

I.4.2 The entropy of mixing

There are three contributions to the entropy of mixing: (a) changes in the vibrational entropy term, (b) terms from changes in magnetic and electronic entropy, and (c) the configurational or statistical term arising from the occupancy of equivalent sites by different chemical species. The last is usually the most important. It arises through statistical mechanics and is fundamentally related to the greater randomness (or loss of information about which ion is on a particular site) in the solid solution compared to the pure end-member.

All substitutions must maintain electroneutrality (balance of formal charges) in the crystal. The substitutions may involve one or more sets of crystallographic sites (sublattices). They may involve ions of like charge, charge coupled substitutions on one sublattice or on several, or the creation or filling of vacant sites.

This structural complexity must be reflected in the thermodynamics of solid solution formation and its subsequent interaction with aqueous solutions. Thus, the crystal chemistry must be understood very well, and various analytical, structural and spectroscopic techniques applied to sample characterisation.

Although thermodynamics offer a macroscopic description, linking thermodynamic properties to the microscopic (atomistic or molecular level) features of the solids insures that the description is not simply and arbitrarily empirical. Such linkage is especially critical if one wishes to extrapolate properties to conditions of pressure, temperature, or composition outside the range where measurements have been made. This is clearly a very important condition when aiming to apply aqueous-solid solution thermodynamics to the performance assessment of nuclear waste repositories. The basic theoretical question is to relate the microscopic details of atomic interactions to site occu-

pancies and macroscopic thermodynamic parameters. The basic practical problem is to obtain useful expressions for the thermodynamic mixing properties of multicomponent solid solutions and to apply them to solid-aqueous phase systems. These practical models should be simple enough to be incorporated into computer codes describing phenomena such as the hydrothermal and geochemical evolution of a nuclear waste repository. They should be robust enough to withstand interpolation and some extrapolation.

I.4.3 Regular, subregular and generalised mixing models

The Gibbs energy of mixing —one of central themes in these Guidelines— can be theoretically analyzed in many ways, the most popular one suggested by Guggenheim (see Part II Chapitre II.1).

For a two-component system, the simplest formulation for $\Delta G_{\mathrm{m}}^{E}(\mathrm{mix})$ (assuming zero excess entropy of mixing) is:

$$\Delta G_{\mathrm{m}}^{E}(\mathrm{mix}) = \Delta H_{\mathrm{m}}(\mathrm{mix}) = \mathrm{R}T\,\alpha\, x_{\mathrm{A}}x_{\mathrm{B}} = W_{\mathrm{H}}\, x_{\mathrm{A}}x_{\mathrm{B}} \qquad \text{(I.4)}$$

where α or W_{H} is the interaction parameter. For a large positive interaction parameter, the model reproduces a symmetric miscibility gap; negative interaction parameter means that the real solid solution is more stable than the ideal one. The end-member activity coefficients can be easily derived from equations like the one above. More complex expressions with even number of interaction parameters result in “asymmetric” mixing models, odd number of parameters —in “symmetric” models (more in Part II).

I.4.4 Dilute solid solutions

Dilute solid solutions represent a practically important case for incorporation of trace elements *Tr* (*e.g.*, radionuclides) into host mineral phases such as calcite, when the mole fraction of *Tr* does not exceed a percent. It can be shown that $\gamma_{\mathrm{Tr}L}$ is approximately constant at trace mole fraction of *Tr*. Thus, at trace mole fraction, the analysis of non-ideal mixing becomes simple because the activity of dilute end-member can be well approximated using Henry’s law. In recognition of this fact, a *dilute solid solutions formalism* has already been applied to solid solutions [1990BAL/PEL], [1992KON/GAM2].

I.4.5 On the relevance of non-ideality

Although the ideality treatment in some Aq-SS has been long controversial, there is a general consensus that two factors mainly control the degree of non-ideality [1975URU], [1996TES/PAN], [1999CUR]:

1/ similarity in size between host and substituting ions and
2/ similarity in crystal lattices.

As an example, Cd^{2+} incorporation to the calcite lattice can be treated as an ideal system since ionic radii of this ion is very similar to Ca^{2+} in calcite, and the crystal classes of pure phases (otavite, $CdCO_3$, and calcite) are the same. Tesoriero and Pankow

[1996TES/PAN] showed that the experimentally measured partition coefficient, *D*, between Cd^{2+} and calcite is close to that calculated if the system is treated as ideal. Conversely, for other cations such as Sr^{2+} and Ba^{2+}, whose sizes are significantly larger than Ca^{2+} and the solid phases (strontianite and witherite, respectively) belong to different crystallographic systems, the partition coefficients differ in more than two orders of magnitude, suggesting strong non-ideality.

The experience acquired from the study of cation incorporation in carbonate and sulphate phases has shown that most Aq-SS systems must be treated as non-ideal systems. This statement leads to a new question, to what extent the SS non-ideality is relevant? The answer depends on the objectives of the study and on the range of concentrations of interest. In the whole range, when all end-members are taken as major, the non-ideality may often cause the formation of intermediate phases due to ordering phenomena (*e.g.*, dolomite in $(Ca,Mg)CO_3$ system) and/or miscibility gaps due to exsolution. Inside of the miscibility gap, at least two solid solution phases with different fixed compositions coexist with the aqueous electrolyte, composition of which is also fixed. Any change in the bulk composition of the Aq-SS system will result upon equilibration only in changed masses of solid phases but in unchanged concentrations of all end-members and aqueous species. Outside the miscibility gaps, the solid solution non-ideality may result in a significant (several times) deviation of dissolved ion concentrations compared to the ideal case. At trace concentrations, the activity coefficients become (almost) constant and simply shift the uptake isotherm up or down, sometimes in 1-2 orders of magnitude if compared to the ideal isotherm for the same end-member.

The following question is also important: What is the right level of complexity of a non-ideal mixing model for the solid solution? The answer depends on the number of end-members and on the accuracy of experimental data used in regression of the interaction parameters of the mixing model. As discussed in Part II, Chapter II.3, the wet chemistry solubility data (K_d, compositions of coexisting aqueous and solid solution phases) usually are so scattered that only one regular interaction parameter (α in Eq. (I.4)) can be determined unequivocally in a binary SS system. In a ternary system, even in the regular model, three binary and one ternary interaction parameters must be determined, which requires a dramatically larger number of experiments which usually is very difficult to produce. On the other hand, the subregular (asymmetric) mixing models, better justified from theoretical viewpoint, can still be parameterised in some suitable Aq-SS systems using the results of galvanic cell measurements which are about 10 times more accurate than the solubility data. Any non-ideal mixing model is difficult to extend on a solid solution system containing more end-members because far more interaction parameters need to be determined.

I.4.6 Solid solution *versus* other uptake modes

Consider a multi-component solid with relatively insoluble end-members in a scenario with a high solid-to-aqueous ratio and short equilibration time. Under these conditions, such a solid may be treated as a pure phase because it is often observed that the dissolution of this solid is congruent during low-temperature reactions while no recrystallisation or precipitation of secondary phases occurs. Thorstenson and Plummer [1977THO/PLU] developed this idea and defined the concept of *stoichiometric saturation*, reviewed in these Guidelines.

In the second case, if the above conditions are not fulfilled, *i.e.*, the solid is able to recrystallise/reprecipitate adjusting its composition due to changes in the composition of the coexisting fluid, the thermodynamic equilibrium between solid solution and aqueous phases can be approached closely.

In the third case, upon the reaction progress, the initial solid solution dissolves until the point when the same solid solution of different composition starts precipitating. This scenario is called *primary saturation*, which is defined as the first ("snapshot" equilibrium) state reached during the congruent dissolution of a solid solution [1978GAR/WOL], [1983DEN/MIC], [1990GLY/REA].

As pointed out by [2000GLY], it is likely that in many natural Aq-SS systems, stoichiometric and primary saturation concepts do not fully explain the observed solubilities of solid solution, rather an intermediate behaviour is observed. An aqueous solution at primary saturation or at thermodynamic equilibrium with respect to a solid solution will be undersaturated with respect to all its pure end-member components.

The second and third cases of Aq-SS behaviour (formation of a new SS of different composition), as well as the co-precipitation of a minor component into a host mineral, may be difficult to discriminate from various sorption processes (adsorption, ion exchange, surface precipitation) on the basis of macroscopic partition data alone. Experiments in such systems often produce linear isotherms which tell nothing about the actual incorporation mechanisms. However, there are some practical criteria that help qualifying the process at least in some systems. A prerequisite for such criteria is that the specific surface of reactive solid is known.

(i) Kinetics and reversibility: adsorption and ion exchange (either on surface or in the interlayer) are relatively fast reactions; in comparison with chemisorption on mineral surfaces, the ion exchange is (almost) reversible. Experiments at high co-precipitation rates may result in weak partitioning of minor component into solid which does not correspond to Aq-SS equilibrium but rather to metastable adsorption states.

(ii) Balance and densities in the surface layer: In most cases, adsorption is limited to a surface monolayer. The maximum amount of metal adsorbed can be estimated from the amount of sorbent, its specific surface, and the site

density parameter. If the measured amount is significantly larger then lattice incorporation or surface co-precipitation processes are probably involved.

(iii) Measurement of the host mineral recrystallisation extent (*e.g.*, with radiotracers). In the case of adsorption or ion exchange, there should be (almost) no recrystallisation. If recrystallisation is significant and amounts to several surface layers (often the case for carbonates) then solid solution is a more likely mechanism than sorption.

(iv) Spectroscopic and microscopic studies, especially surface-sensitive, can support mechanistic interpretation of the macroscopic data either as surface-dependent uptake (adsorption, surface precipitation) or (layer) volume uptake (ion exchange, solid solution formation).

(v) Volume uptake mechanisms such as ion exchange in clays or zeolites can be modelled using either the solid solution concept or the (ad)sorption concept based on the capacity (surface site density) parameter. In this case, the (pore) surface- volume relationships must be known.

One must keep in mind that for most of the applications of interest in radioactive waste management, the radionuclides of concern will occur at rather small concentrations compared to the major components in the Aq-SS systems. In this context, the incorporation of radionuclide trace components into a host solid solution can be approached quasi-ideally, and the partition of trace radionuclides can be approximated by Henry's Law with conditional solubility products established as shown in Section II.1.1.4.1. Advantage of this simple approach is that no information about surfaces or pore volumes is needed, only the amount of reacted host mineral must be known.

I.4.7 Concepts and approximations in geochemical modelling of Aq-SS systems

As already mentioned in Section I.1.3, these Guidelines are intended to provide a scientific background for incorporating solid solution and Aq-SS concepts and data in the geochemical models used in performance assessment studies. To this end, two different approaches can be used depending of the existing data: the *forward* and *inverse modelling*.

Forward modelling consists of the prediction of concentrations (or activities) of chemical species in solution and of solid phases in a system under specific temperature and pressure conditions. In most codes, this type of models is based on the law of mass action (LMA) formalism. Most of the geochemical code packages used in PA related calculations are of this kind, *i.e.*, PhreeqC, EQ 3/6. Aq-SS systems can be treated in these codes to a limited extent (see Part II, Section II.1.2.3); solving Aq-SS equilibria with LMA codes is, in general, not a straightforward process because a single aqueous speciation calculation turns into a series of many runs controlled by non-rigorous test

procedures, without a theoretical guarantee of convergence to a unique solution. The only case which is easy to solve with LMA methods is the stoichiometric saturation state [1990GLY/REA] in which the solid solution is treated as a pure (fixed-composition) solid phase.

Inverse modelling is usually performed for determining some input parameters (*e.g.*, solubility products, initial system composition) provided that some output parameters (*e.g.*, dissolved concentrations, or mole fractions in equilibrium) are measurable and available. In the case of Aq-SS systems, inverse modelling may help to determine values of activity coefficients, interaction parameters, standard Gibbs energies and/or solubility constants of end-members. The available codes to perform extended inverse modelling calculations in Aq-SS systems include the GEMS-PSI package (see more in Part II, Section II.1.3).

I.4.7.1 Lippmann diagrams, a tool to visualise binary Aq-SS systems

Binary Aq-SS systems are, in fact, ternary systems in which two components are solid mixture end-members, and one component is the aqueous electrolyte solution. The latter is always in excess, therefore such systems are often called "pseudo-binary" or simply "binary" because they involve a binary solid mixture. In geochemistry and aquatic chemistry, the Lippmann phase diagram [1977LIP], [1980LIP], [1982LIP] became a popular tool for analysing pseudo-binary Aq-SS equilibria after papers by [1990GLY/REA], [1990GLY/REA2], enhanced with the MBSSAS code [1991GLY] for computing/plotting such diagrams, retrieving Margules parameters and equilibrium relations. This work has been extended and deepened by [1992KON/GAM], [2000GAM/KON], [2000PRI/FER]. A full description of the development and application of Lippmann diagrams is given in Part II, Section II.1.2.2.

Several illustrative examples of the theory and application of Aq-SS to trace elemental (radionuclide) solubility are developed in Part II.3.

I.4.8 Kinetic and thermodynamic approximations to Aq-SS in geochemical reactive transport modelling

Recently Lichtner and Carey [2006LIC/CAR] have presented a promising approach in order to link the kinetics and thermodynamics of solid solution formation into reactive transport modelling.

The method is applicable to problems involving advective, dispersive, and diffusive transport in a porous medium. The authors represent the continuously variable solid solution composition by a discrete set of stoichiometric solids that cover the composition range and they combine it with a kinetic formulation of the rates of reaction. In this way a spatial and temporal evolution of the solid solution concentration and composition is obtained. Lichtner and Carey [2006LIC/CAR] have demonstrated that equilibrium of an aqueous solution with a stoichiometric solid derived from a solid solution

corresponds to equilibrium of the solid solution itself if and only if equilibrium of the stoichiometric solid is stable. One advantage of this approach is that it is unnecessary to introduce any additional compositional variables to represent the solid solution. A major consequence of this kinetic discrete-composition solid solution representation is that modelling solid solutions is similar to modelling pure mineral phases with the exception of a weighting factor applied to reaction rates of stoichiometric solids corresponding to a common solid solution. With this approach, precipitation leads to a discrete zonation of the solid solution that approximates the continuous variation in composition expected for the actual solid solution. The approach is demonstrated for a hypothetical ideal and non-ideal binary solid solution $A_xB_{1-x}C$.

Recently, we have [2006AYO] implemented this Lichnter formalism in the Retraso reactive transport code with quite promising results.

I.5 Experimental and analytical aspects

Thermodynamics of solid solution-aqueous solution (Aq-SS) systems is relatively well established on theoretical side (see Chapter II.1) [2000GAM/KON], [2000GLY], [1990GLY/REA], [1980LIP] and advanced numerical methods have been developed to describe such systems quantitatively (see Chapter II.2). However, applying these concepts successfully to *real world* problems requires actual thermodynamic data as a baseline for geochemical modelling. Such thermodynamic data can be obtained either from laboratory experiments with synthetic compounds or from analysis of naturally occurring solid solution phases. Here, the focus will be on how to derive thermodynamic data from co-precipitation experiments using synthetic systems at relatively low (waste repository relevant) temperature $T < 373$ K. There will be some emphasis on high temperature synthesis as well as on samples from natural systems.

Characterising the aqueous solution and the solid phase on mineralogical and molecular levels is a prerequisite for deriving thermodynamic data. It is also crucial to prove that the Aq-SS system represents equilibrium conditions. Furthermore, synthesising solid solution phases from aqueous solution involve various potential pitfalls which need to be identified before one starts to interpret experimentally obtained data in terms of Aq-SS thermodynamics. Therefore, the intention of Chapter II.2 is to provide a critical overview of analytical techniques which are typically used to characterise the aqueous solution and the solid solution phase and how one obtains raw data usable for the thermodynamic description of such a system.

First of all, synthesis procedures, as well as some fundamental aspects of co-precipitation experiments in aqueous solution, will be discussed. Special emphasis will be on actinides and fission products in the trace level concentration range.

I.5.1 Synthesis procedures

Probably the most common way to synthesise solid solution phases is by simple ***batch type*** experiments where the host solid phase (major component) is supersaturated. This is done by mixing two different components to produce the solid phase and a trace component to co-precipitate. Normally, these kinds of experiments produce chemical zonation and logarithmic distribution laws (Doerner-Hoskins). Potential experimental approaches to minimise these effects are explain in full detail in Section II.2.1.1.1, they include ***batch-type constant composition methods***, and ***counter-diffusion experiments*** [1997PRI/FER], [1993PRI/PUT]. Many of the drawbacks involved in the above-mentioned techniques can be overcome by performing co-precipitation experiment in a ***mixed flow reactor.*** With respect to experimental studies on Aq-SS systems, it seems crucial that one understands the involved reaction mechanisms that occur throughout an experiment on a molecular level. In particular, when working under low (room)-temperature conditions in aqueous systems, kinetic effects, the formation of precursor phases and the metastability effects have to be critically taken into account before using experimental results for determining thermodynamic data. The synthesis procedure will ultimately depend on the final objective of the solid solution to be investigated.

I.5.2 Characterization of the solid solution

As we have repeatedly pointed out, the characterisation and determination of the resulting solid phase at molecular or even atomic level is a fundamental prerequisite for the establishment of the appropriated sorption mechanism and consequently for the determination of the thermodynamic properties of the Aq-SS.

The following table gives a brief account of the presently existing techniques to characterise solid solutions. This is at present a very dynamic research and more and better techniques are becoming available these days.

Table I-1: Overview of some selected analytical techniques to obtain key information of solid solution phases

Mineralogical composition	***Phase identification, element concentrations, compositional homogeneity***
ICP-AES/MS (Inductively Coupled Plasma−Atomic Emission Spectrometer/Mass Spectrometer)	ICP-AES/MS provides element concentrations down to the ultra trace concentration range.
SEM (Scanning Electron Microscopy), TEM (Transmission Electron Microscopy), EM (Electron Microprobe)	SEM, TEM, EM can provide spatially resolved chemical analysis.
XRD (X-ray Diffraction)	XRD allows identification of solid phases (based on known crystal structures).
Speciation	***Characterisation of redox state and identification of molecular species***
XAS (X-ray Absorption Spectroscopy) XANES (X-ray Absorption Near Edge Structure)	The XANES region in a X-ray absorption spectrum provides information about the redox state (valence shift) in the sense of fingerprinting.
TRLFS (Time Resolved Laser Fluorescence Spectroscopy)	TRLFS provides information about the coordination sphere of certain radionuclides. Fluorescence energy and associated life time can be analysed independently. Changes in the peak maxima of the emission spectra indicate a change in the chemical environment or ligand field. Changes in the life time indicate the presence of quenchers such as H_2O or OH^- molecules in the 1st coordination sphere.
Structure	***Lattice constants and associated long-range order (LRO) and short-range order (SRO) phenomena***
XRD (X-ray Diffraction)	Characterisation of long-range order phenomena (*e.g.*, lattice constants, superstructures) and site occupancies based on powder or single crystal measurements.
XAFS (X-ray Absorption Fine Structure) EXAFS (Extended X-ray Absorption Fine Structure)	XAFS spectroscopy provides information about SRO phenomena. The XANES region contains information about coordination geometry and orientation. The EXAFS region provides information about bond lengths, coordination numbers and type of coordinating atoms (EXAFS equation).
NMR (Nuclear Magnetic Resonance)	NMR spectroscopy provides information about local coordination environment of a nuclide, based on differences between allowed spin states of atomic nuclei.
Thermodynamics	***Thermodynamic mixing properties (e.g., entropy, enthalpy, heat capaciy)***
Calorimetry	Measurement of heat capacities and heats of phase transitions (thermophysical measurements) and measurement of heats of reaction (thermochemical measurements).
Electrochemical measurements	The electrochemical potential between well defined aqueous-solid solution systems can provide directly thermodynamic data on solid solution-aqueous solution equlibria.

I.5.3 Solubility measurements in aqueous solutions

The natural way to experimentally characterise Aq-SS equilibria is by means of solubility measurements. In contrast to solubility studies of pure compounds, the solubility measurements in Aq-SS systems potentially involve a number of experimental complexities that have to be fully assessed prior to the data interpretation. In Section II.2.2, three solubility concepts for Aq-SS systems are introduced and discussed for a simple binary (B,C)A system —*e.g.*, (Ba,Sr)SO_4, Barite-Celestite:

(1) Thermodynamic equilibrium,

(2) Primary saturation and

(3) Stoichiometric saturation.

The graphical interpretation of Aq-SS solubility experiments in quasi-binary systems (two solid end-members and the aqueous phase) can be done by applying Lippmann diagrams based on the total solubility product ΣΠ [1990GLY/REA].

The main difficulty arising from direct solubility measurements of Aq-SS systems concerns the evolution and the determination of the resulting solid solution phase(s) which may form as a result of putting in contact an initial solid solution phase with an aqueous solution. Upon the incongruent dissolution of the initial solid solution phase, secondary phases may form. In this context, much care has to be taken in order to ensure that the solid solution under study has been properly characterised, otherwise the resulting thermodynamic data can be wrong. Various spectroscopic techniques available for the characterisation of solid solutions are described in the following section and more extensively in Chapter II.2.

Additionally, once the resulting solid solution phase is well characterised the required precautions have to be put in place when dealing with the measurement and determination of the resulting aqueous solution. In this respect we submit the reader to the appropriated Guidelines of the NEA TDB project concerning solubility determinations and ionic strength corrections [1999NEA].

I.5.4 Partition/distribution experiments

Partition experiments are a specific variation of solubility measurements in Aq-SS systems, which have been largely used in the past and form the basis for the initial description of homogeneous and heterogeneous (logarithmic) distribution laws as a means to quantify sorption/uptake of trace components. In this case, the emphasis of the experimental determination resides on the trace component concentration in the solid and in the aqueous phases, because the distribution coefficient is usually defined as the ratio of both.

Two different experimental setups were used. (1) *Co-precipitation uptake:* the trace component is co-precipitated with a certain host solid (*i.e.*, calcite), and the distribution of the trace component between the solid and the aqueous phase is monitored as

a function of time and initial trace component addition in the system. (2) *Recrystallization uptake*, when a spike of the trace component is introduced into an already equilibrated Aq-SS system, and the distribution of the trace component is monitored as a function of time and aqueous trace element concentration.

Most past experiments of either type (1) or (2) were not supported by the appropriate spectroscopic characterisation of the resulting solid phases and, therefore, no conclusive data on the incorporation mechanisms can be derived from the partition experiments alone. There are, however, notable exceptions, where the distribution data is complemented with proper spectroscopic characterisation of the trace component bonding environment in the solid phase [1989WER/CHA]. In this case, the distribution data can be used to derive the thermodynamic properties of solid solution end-members.

More detail on the development and shortcomings of distribution experiments is given in Chapter II.2.

I.5.5 Direct measurements of thermodynamic and mixing properties of solids in Aq-SS systems

I.5.5.1 Retrieval of excess Gibbs energy from electrochemical measurements

The difference between the chemical potentials of pure solid and its solid solution with another end-member in (metastable) equilibrium with aqueous solutions of the same ionic strength and with the same atmospheres can be determined using emf measurements in two or three interconnected electrochemical cells ([1990KON/GAM], [1994ROC/CAS], [1998MCB/ROC]). Such experiments yield results that are much more precise than any results of "classic" solubility measurements (Section II.2.2), which has been demonstrated for the (Mn,Co)CO_3-aqueous system by Königsberger and Gamsjäger [1990KON/GAM] and for the (Ca,Cd)CO_3-aqueous system by Rock *et al.* [1994ROC/CAS] and McBeath *et al.* [1998MCB/ROC]. The latter paper also contains a detailed description of the experimental setup with measured, intermediate and final calculated data, as well as a discussion of the advantages of the direct electrochemical methods compared to solubility measurements. They are thoroughly discussed in the appropriated section of Chapter II.2.

I.5.5.2 Calorimetry

Calorimetry, the measurement of heat effects, is a fundamental tool of experimental thermodynamics. It provides data on heat capacities, entropies, and enthalpies and is thus complementary to solubility and other equilibrium measurements that provide Gibbs energies. Calorimetric data is being extensively used in the derivation and validation of thermodynamic data and cycles through out the NEA TDB project. Guidelines [1999PUI/RAR] contain information about how to use calorimetric data in general.

Here, we will emphasize the use of calorimetric data to derive thermodynamic properties of Aq-SS.

Broadly speaking, calorimetry can be divided into two categories: the measurement of heat capacities and heats of phase transition within a material of constant composition and the measurement of heats of reaction. Sometimes the first category is called "thermophysical" and the second "thermochemical" measurement.

Cryogenic adiabatic calorimetry [1972ROB/HEM2] is the most accurate method for measuring low temperature heat capacities but it requires several grams of sample. In general, the instruments are custom built and the work is performed in a small number of specialised laboratories. It is capable of determining heat capacities with an accuracy of 0.1 - 0.5% and standard entropies with an accuracy of 0.5 - 1%.

Differential scanning calorimetry (DSC) [1992BOE/CAL], [1982STE/WEI] provides heat capacity measurements from about 100 to 1700 K, with accuracy ranging from about 1% near room temperature to 3 - 5% at the highest temperatures [2005MOR/NAV]. Many commercial instruments are available for the range 100 to 1000 K, and several for higher temperatures. Differential thermal analysis to 2773 K can provide enthalpies of phase transitions with an accuracy of about 5 - 10% at the higher temperatures [2005NAV/BEN]. Drop calorimetry (sample of 10 - 100 g) dropped from a high temperature furnace into a room temperature calorimeter provides the heat content ($H_T - H_{298}$), differentiation of which gives the heat capacity [1982STE/WEI]. Accuracy is 0.5 - 1% in the best cases.

Despite the apparent maturity of the field of heat capacity measurement, the available data for end-member and solid solution phases relevant to nuclear materials are surprisingly incomplete. Many of the older data, used to calculate standard entropies of common materials, in fact rely on extrapolations from 50 K to absolute zero and also suffer from sample characterisation inadequate by modern standards. There are still relatively few studies of solid solutions, and researchers in this field are encouraged to use calorimetry to establish the basic thermodynamic properties of solid solution phases.

To obtain the heat of formation of a material, a chemical reaction must take place in a calorimeter which relates that phase to products of known thermodynamic properties. That reaction may be direct, as in reaction calorimetry of a metal to a sulphide [1988BRY/KLE] or indirect, involving a process in which reactants and products are each converted to the same final state, and a thermodynamic cycle is written to relate their enthalpies. This final state often involves the dissolution of the solids in an appropriate solvent, which can range from water or aqueous acid [1972ROB/HEM2] to a molten oxide at high temperature [1977NAV], [1997NAV]. Because many of the solids relevant to nuclear materials are not readily soluble (in terms of both solubility limits and kinetics of dissolution) in aqueous solvents near room temperature, the latter

route, high temperature oxide melt solution calorimetry, has proven very useful [1977NAV], [1997NAV].

I.6 Testing the Aq-SS concepts and methods in nuclear waste management relevant systems

One of the main objectives of this work is to determine to which extent the current status of the thermodynamics of Aq-SS can be integrated in the models and sub-models used in the Performance Assessment of nuclear waste repositories. To this end we have compiled a number of test cases that are fully developed in Chapter II.3. What follows is a summary of the cases and their main findings.

I.6.1 Radium and its incorporation into the barite solid solution family: environmental implications

I.6.1.1 The radium-barite relationship in natural and anthropogenic environments

Perhaps, the co-precipitation between radium isotopes and barite precipitates is one of the best known examples. Dozens of studies on several scientific disciplines have established a link between the concentration of radium and the precipitation of barite, since the work of Doerner and Hoskins in 1925 [1925DOE/HOS], from which the theory of growth as incremental layers was defined (*Doerner-Hoskins logarithm distribution law*, Doerner and Hoskins, 1925). Radium is divalent and has an ionic radius (1.43 Å) quite similar to the Ba^{2+} one (1.36 Å), so that it is expected to be well accommodated in the barite lattice.

The role of barite as solubility-controlling phase of radium has been proposed in natural and in *anthropogenic* environments. Radium-bearing barite is present in uranium mill tailings [1987NIR]. Uranium is concentrated from ore minerals by leaching with acid sulphuric. Due to its relative low mobility during leaching conditions, radium is accumulated in the fine fraction of the waste, which is eventually stored in mill tailings. From these tailings, radium may be released to the soil, resulting in a serious concern due to its high radioactivity. The mobility of radium after storage have recently been evaluated by Martin and Akber [1999MAR/AKB] and Martin *et al.* [2003MAR/CRU]; Martin and Akber [1999MAR/AKB] used the relative concentrations of radium isotopes to evaluate the absorption/desorption of radionuclides and secondary mineral formation in groundwater systems close to uranium mine tailings. Their data indicated that almost all ^{226}Ra was removed by the formation of barite solid solution. On the other hand, Martin *et al.* [2003MAR/CRU] concluded that dissolution of a solid $(Ba,Ra)SO_4$ solid solution controls the aqueous concentration of radium and barium in waste porewater, confirming previous data by Snodgrass and Hileman [1985SNO/HIL].

I.6.1.2 Numerical modelling involving (Ba,Ra)SO_4 solid solutions

As already indicated in the previous section, the seminal work of Doerner and Hoskins on this system ([1925DOE/HOS]) was crucial to establish the basic principals of solid solution precipitation from aqueous solution and the development of the logarithmic distribution law. This is based on the experimentally proven assumption that the [Ra(II)]/[Ba(II)] ratio in the surface layer is proportional to their ratio in aqueous solution. As the composition of the aqueous phase changes with time as a result of the changes in the elemental composition, so does the composition of the crystal surface, leading to the so-called logarithmic distribution law (see details in Chapter II.3).

More recently, Langmuir and Riese [1985LAN/RIE] used empirical distribution coefficient data to derive Gibbs energies and enthalpies of solid solution of Ra(II) into various alkaline earth sulphate and carbonate minerals and established some interesting trends in the stability of these solid solution phases. According to this study, the distribution of Ra(II) into these minerals decreased in the following order: anhydrite > celestite > anglesite > barite > aragonite > calcite > strontianite > whiterite > cerussite.

In a recent work, Zhu [2004ZHU2] implemented the thermodynamic and kinetic data of the (Ba,Ra)SO_4 solid solution system in reactive transport codes (EQMOD, [1992YEH], and PHREEQC, [1999PAR/APP]) and compared the data obtained when considering pure phases and solid solutions. The approach by Zhu, included aqueous speciation and complexation, thermodynamic properties of solid and aqueous solutions and precipitation and dissolution kinetics. The obtained results clearly showed that Ra^{2+} concentrations in water differ several orders of magnitude whether equilibrium with a solid solution is considered or not. In one of these models, an oil-field brine was simulated to cool down from 100 to 25 ºC over five days. The numerical outcome showed a quick precipitation of a (Ba,Ra)SO_4 solid solution, implying a significant decrease of radium in solution. During the precipitation process, the solution was undersaturated with respect with pure $RaSO_{4(cr)}$.

Berner and Curti [2002BER/CUR] used the GEM approach (see Section II.1.2.4) to calculate the retention of radium in a nuclear waste repository hosted by the Opalinus Clay. Their results showed that the solubility limit in the clay porewater considering the "conventional" approach, *i.e.*, the total concentration of dissolved radium being controlled by the least soluble pure phase ($RaSO_{4(c)}$), was 4.8×10^{-8} M. In contrast, the co-precipitation of radium into ideal solid solution with barite lowered the solubility limit to 8.2×10^{-12} M. The solubility limit for Ra was even lower, 7×10^{-13} M, when a more complex Aq-SS system involving gypsum, barite and celestite $SrSO_4$ solid solutions was considered. When both barium sulphate and carbonate were present in the system, Ra^{2+} was almost exclusively partitioned into barite due to much higher solubility of witherite (Ba carbonate).

The consequences of the $RaSO_4$(s)-$BaSO_4$(s) solid solution formation for reactive transport modelling of Ra(II) in clay environments are further explored in some calculations performed in Section II.3.1.2.

I.6.1.3 Conclusions

Formation of $RaSO_4$(s)-$BaSO_4$(s) solid solution is well documented in both natural and anthropogenic environments. The Aq-SS equilibria have been largely investigated in well controlled laboratory systems and there are both macroscopic and spectroscopic investigations of the resulting solid solution formation. Both direct and inverse modelling techniques have been used to describe its behaviour and coupling of this Aq-SS to reactive transport codes has been successfully done. The outcome of it is that the predicted Ra(II) solubilities are substantially lower than the ones predicted by using the individual solubility of $RaSO_4$(s). In this context, it constitutes a clear case for the application of Aq-SS thermodynamics for PA.

The results from the $(Ba,Ra)SO_4$ Aq-SS system strongly support the idea that the knowledge of Aq-SS systems is essential when evaluating the behaviour of radionuclides in PA. Conventional numerical models failed in reproducing environmental data because most codes still use pure phases as solubility-controlling components

I.6.2 Cement phases – Solubility of calcium silicate hydrates (C-S-H)

I.6.2.1 Relevance of cement phases in radioactive waste management

Ordinary Portland Cement (OPC) is the most widespread matrix material currently considered in disposal of low-to-intermediate level nuclear (and non-nuclear) waste ([1992BER], [1992REA], [1997GLA]).

Ca. 60% of hydrated OPC consist of the *calcium silicate hydrate* phase (C-S-H in cement chemistry notation, where CaO is denoted as C, SiO_2 as S, and H_2O as H) of variable composition expressed with the C/S (Ca/Si molar) ratio, usually in the range $0.8 < C/S < 1.7$. The structure and stability of C-S-H has been the subject of a long debate because C-S-H is a major binder in the hydrated cement paste, and because it can immobilise many hazardous elements. The C-S-H structure is flexible enough to accommodate variable fractions of calcium and to provide exchange sites for various cations (Na, K, Cs, Sr, Al, Zn, …) and, consequently, to bind additional metals and radionuclides in their structures.

I.6.2.2 Thermodynamic modelling of C-S-H and its limitations

In principle, if the end-member properties are known, thermodynamic modelling can calculate stable phase assemblages and the resulting metal partitioning between phases as a function of physicochemical conditions and bulk composition of the system. How-

ever, the $CaO\text{-}SiO_2\text{-}H_2O$ system poses special problems to thermodynamic modelling when C-S-H phases are involved. The C-S-H "gel" is, in fact, a less-polymerised metastable precursor of crystalline tobermorite or jennite, and it tends to convert into a more polymerised form with time or at elevated temperatures. C-S-H phases have significant and variable specific surface area (up to 200 $m^2 \cdot g^{-1}$ or more) which makes them quite reactive, prone to incongruent dissolution with preferential release of Ca upon acidification or carbonation of the system, or even upon decreasing solid/water (S/W) ratio, which leads to precipitation of more silica-rich secondary (but again metastable) C-S-H phases. This kind of incongruent, non-stoichiometric dissolution behaviour, typical for Aq-SS equilibria, must be duly addressed in any experimental work or physico-chemical modelling related to cement-water interactions.

Kulik and Kersten [2001KUL/KER] have identified two alternative ways to perform the thermodynamic modeling of partial-equilibrium Aq-SS systems such as $C\text{-}S\text{-}H\text{–}H_2O$.

(i) By assuming end-member stoichiometries derived from stable mineral analogs such as tobermorite, jennite, or portlandite, and eventually include non-ideal behavior into solid solutions formed by these end-members, if this is needed for fitting experimental solubility data.

(ii) By seeking for such C-S-H end-member stoichiometries and their standard molar Gibbs energy G^{o}_{m} (298.15 K) values that would make possible to apply the ideal solid solution approach.

However, the need for a further extension to describe trace metal or radionuclide (*i.e.*, multi-component) C-S-H systems makes the first approach (i) not possible in practice due to the necessity to introduce many more (semi-empirical) interaction parameters with little hope to collect enough experimental data for finding parameter values with reasonable precision. For those reasons, the second approach (ii) based on optimisation of end-member stoichiometries to fit experimental data appears to be the only practically feasible opportunity [2001KUL/KER][2006LOT/WIN].

These authors have shown that the behaviour of C-S-H Aq-SS system can be reduced to ideal by the appropriated scaling of the end-member stoichiometries.

I.6.2.3 Geochemical modelling of C-S-H systems of interest in radioactive waste management

The validity of this approach has been tested by applying the GEMS-PSI code and database to the C-S-H solubility data derived in the experiments by [1965GRE/CHA], which, in principle, fulfil the necessary requirements for Aq-SS solubility data. The result of this validity test in terms of reproducing the dissolved Ca and Si concentrations, as well as the pH data, are quite encouraging and cover the full $0 < C/S < 1.7$ compositional range (more in Section II.3.2.)

The C-S-H ideal solid solution model has been further extended [2002KUL/KER] to incorporate a trace metal end-member for the case of Zn, where limited solubility data are available [1999JOH/KER]. The limitations on available thermodynamic data for Zn-Ca silicates and Zn-C-S-H end-member phases has been overcome by using dual-thermodynamic calculations (see Section II.1.3.2) in order to estimate the appropriated end-member stoichiometries and their associated thermodynamic properties.

I.6.2.4 Conclusions

The examples developed in Section II.3.2 show the potential of multicomponent ideal solid solutions to model the Aq-SS C-S-H system and the incorporation of cations in the ill-defined gel structures. Future work is going to be devoted to extend the applicability of this approach to increase amount of experimental data being reported for the sorption of Na, K, Al, Sr and Cs in these systems.

I.6.3 Structural incorporation of trivalent actinides/lanthanides into Calcite

I.6.3.1 The relevance of calcite for radioactive waste management

Calcite is a ubiquitous mineral phase in most geological environments, and it is particularly abundant in clay rocks like the ones forming the Opalinous clay in Switzerland (up to 11% content) [1998BRA/BAE] and in the Bure argillite [2001AND]. It is also a key secondary phase in cementitious materials. Consequently, radionuclide sorption processes in calcite comprise an important component of the migration models used in performance assessment of nuclear waste repositories.

In this particular context, we will be interested to investigate the co-precipitation/solid solution formation processes related to the interaction of actinides and lanthanides with the calcite structure.

Co-precipitation of various trace metals with calcite has been extensively studied through the years. The review work performed by Curti [1999CUR] constitutes a good compilation of the main studies up to 1998, although much information has been generated since then. As pointed out in [2000GLY], there is a substantial amount of thermodynamic data for divalent metal incorporation into calcite. In addition, sorption studies of U(VI), Th(IV), Np(V), Pu(V)/Pu(VI) and Cm(III) on calcite have been reported [1992CAR/BRU], [2005MAR/STU], [1982SHA/MOR], [2002STU/FAN2] and [2005ZAV/ROB].

The main focus of this test case will be on experimental studies of the structural incorporation of trivalent f-elements, primarily Pu(III), Am(III) and Cm(III).

I.6.3.2 Macroscopic information related to the sorption of f-elements into calcite

There is a substantial amount of experimental information concerning the partition of lanthanides and trivalent actinides in the calcite/aqueous solution system. The lanthanide most extensively studied has been Eu(III). The macroscopic information has been mainly rationalised in terms of distribution coefficients indicating the following general patterns:

1. Experiments by Lakshtanov and Stipp [2004LAK/STI] at pH about 6 indicate that the partition of Eu(III) is not much affected by the precipitation rate. A similar observation (in seawater at pH about 8) was made by Zhong and Mucci [1995ZHO/MUC].

2. Distribution coefficients derived in [1995ZHO/MUC] indicate a positive dependence with the total lanthanide concentration in aqueous solution. For Eu(III), the partition coefficient $k_D = (x_{Me} \cdot [Ca]) / (x_{Ca} \cdot [Me])$ ranged from 200 at dissolved concentration [Eu(III)] = 10 nM to k_D = 1400 at [Eu(III)] = 170 nM. The distribution coefficients reported in [2004LAK/STI] are $k_D = (770 \pm 290)$ in the [Eu(III)] range from 0.1 to 6.9 nM.

3. Zhong and Mucci [1995ZHO/MUC] observed a correlation between the lanthanide content in calcite with the $[Na^+]$ in the artificial seawater they used in their experiments. This was not observed by Lakstanov and Stipp [2004LAK/STI].

4. The reaction mechanism proposed in [1995ZHO/MUC] implied the following substitution reaction at the solid phase: $2Ca^{2+} \rightleftharpoons Na^+ + Eu^{3+}$.

5. The proposed mechanism in [2004LAK/STI] implied the combined reaction substitution $3Ca^{2+} \rightleftharpoons 2Eu^{3+} + vac_{calcite}$ (vacancy site in the calcite structure), together with the substitution reaction $2Ca^{2+} \rightleftharpoons Eu(OH)_2^+$

I.6.3.3 Spectroscopic information on the incorporation of f-elements into the calcite structure

This can be summarised as follows:

1. EXAFS studies by Elzinga *et al*. [2002ELZ/REE] indicate that the investigated lanthanides occupy a Ca site within the calcite structure. For Dy and Yb they observed the expected 6-fold coordination, while Nd and Sm appear to be 7-fold coordinated and with longer Nd-O and Sm-O distances than expected by the sum of the respective ionic radii. A similar observation is made for the Nd(III) calcite system in EXAFS by Whiters *et al.* [2003WHI/PEA], and their near IR studies brought them to suggest the incorporation of $NdOH^+$ into the calcite structure.

2. The TRLFS studies by Marques-Fernandes *et al.* [2005MAR/STU] indicated that Cm(III) is truly incorporated into the structure and that two incorporated species may be distinguished. The spectroscopic data is consistent with substitution reactions previously discussed.

I.6.3.4 Thermodynamic modelling of the Eu(III)/calcite system

Curti *et al.* [2005CUR/KUL] have recently performed a thermodynamic modelling of the Eu(III)/calcite Aq-SS system . The data used was a combination of batch type sorption experiments at high pH = 13 and the data from [1995ZHO/MUC] and [2004LAK/STI].

It was not possible to fit all the data to a simple quasi-binary Aq-SS system with the end-members $CaCO_3$ and Eu_2CO_3 or $EuNa(CO_3)_2$. However, the results from the DualTh GEM modelling (see Section II.1.3.2 for more details) indicated a good fit by assuming the following three end-members EuO(OH), $EuH(CO_3)_2$ and $CaCO_3$. This would indicate the incorporation of two different Eu species in the calcite lattice, one involving the substitution of $2Ca^{2+}$ by Eu^{3+} and H^+, and another, the incorporation of the Eu(III)-hydroxo moiety. This implies a significant relaxation of the calcite structure with a Eu^{3+} 9-fold coordinated. The modelling results have not been directly verified by spectroscopy although they are consistent with recent TRFLS observations.

I.6.3.5 Conclusions

There is a large body of macroscopic chemical data regarding the sorption of lanthanide and trivalent actinide elements into calcite. The spectroscopic data so far available would indicate that trivalent lanthanides and actinides are incorporated into the calcite structure and in two different forms. However, there is no consensus about the precise substitution mechanisms involved. The inverse thermodynamic modelling done by using the dual-thermodynamic approach indicates that a consistent Aq-SS model can be derived for this system which accounts for most of the Eu(III)/calcite partition data published in the literature.

I.6.4 Solid solutions in the nuclear fuel cycle

I.6.4.1 The applicability of Aq-SS thermodynamics to spent nuclear fuel

The nuclear fuel cycle constitutes one of the areas where the applicability of Aq-SS thermodynamics becomes most relevant. Most of the components involved from cradle (mineral phases in uranium ore deposits) to grave (spent nuclear fuel and other immobilising matrices) can be considered as solid solutions.

There has been a large amount of research effort directed to characterise and amount and location of the various radionuclides in the UO_2 spent fuel matrix. This has led to the application of Aq-SS concepts and models to interpret the various processes

governing the dissolution behaviour of the various radionuclides from the spent fuel matrix.

I.6.4.2 Main results from the characterisation of UO_2 spent nuclear fuel

The key observations regarding the evolution of the occurrence and location of radionuclides from the large amount of information collected so far (for details, see Section II.3), are as follows:

Processes occurring when irradiation increases [1988KLE3]:

1. Increase in the relative concentration of fission products.
2. Changes (decrease) in the oxygen to metal ratio and the oxygen chemical potential.
3. Existence of radial variations in the fission product concentrations due to thermal gradients.
4. Decay of β-active fission products.

The resulting fission products can be classified in the following groups according to the nature of the phases where they are hosted in the spent fuel matrix:

1. Fission gases (Kr, Xe, Br, I);
2. Metallic phases (Mo, Tc, Ru, Rh, Pd, Ag, Cd, In, Sn, Sb, Te);
3. Oxide phases (Rb, Cs, Ba, Zr, Nb, Mo and Te) and
4. Solid solutions in the fuel matrix (Actinides, Lanthanides, Sr, Zr and Nb).

I.6.4.3 Application of Aq-SS thermodynamics to spent fuel dissolution data

The stoichiometric saturation concept as postulated by Thorstenson and Plummer [1977THO/PLU] and defined by [1990GLY] has been applied to some of the dissolution data of those fission products that have been identified to be present as solid solution in the UO_2 matrix. The stoichiometric saturation approach is well suited to be applied to the spent fuel system as it explains the behaviour of Aq-SS that are not in true equilibrium.

The general dissolution mechanism is as follows: by assuming that the minor radionuclides are dissolving congruently with the UO_2 matrix the radionuclide concentration in solution can be related to the uranium concentration in solution by the molar fraction of the radionuclide in the spent fuel solid solution.

This approach has been applied to a number of carefully performed spent fuel dissolution studies [1999BRU/CER] and [2003BRU/CER]. The details of the thermodynamic modelling are given in Section II.3. What follows is a summary of the main findings:

For Sr(II) the observed aqueous concentrations can be reproduced for all those spent fuel experiments which are sufficiently away from saturation, in the Sr concentration range $1 \cdot 10^{-9}$ to $1 \cdot 10^{-7}$ mol·dm^{-3}.

For Np, the observed aqueous concentrations can be reproduced for the data collected away from saturation, in the Np concentration range $1 \cdot 10^{-9}$ to $1 \cdot 10^{-8}$ mol·dm^{-3}. At higher concentrations the saturation with respect to $Np(OH)_4(s)$ was apparent.

For Pu a similar behaviour was observed in the concentration range $1 \cdot 10^{-9}$ to $1 \cdot 10^{-8}$ mol·dm^{-3}.

For the lanthanides, Eu(III), Sm(III), Gd(III) and La(III) the observed aqueous concentrations could be explained by the stoichiometric saturation model in the concentration range $1 \cdot 10^{-10}$ to $1 \cdot 10^{-7}$ mol·dm^{-3}.

I.6.4.4 Conclusions

The combination of a substantial solid characterization effort together with the dissolution data properly conducted has enabled the application of the stoichiometric saturation approach to model the Aq-SS behaviour of a number of radionuclides that are known to be present in solid solution in the spent fuel matrix.

I.7 Report conclusions

The main conclusions arising from this contribution are the following:

1. Aqueous-Solid Solution (Aq-SS) systems are ubiquitous in nature and therefore intrinsic to the understanding and quantification of radionuclide containment and retardation processes represented in Performance Assessments for geological repositories.
2. The partition behaviour of trace elements in general and radionuclides in particular is the result of a number of uptake (sorption) processes that range from adsorption and ion exchange to structural incorporation and solid solution formation. Molecular spectroscopic methods have to be used to properly qualify and understand these processes quantified in macroscopic partition experiments.
3. Thermodynamics of Aq-SS systems is an established discipline and most of the conceptual framework is solidly built. However, there is a lack of fundamental thermodynamic data that prevents its use in a more consistent way. Experimental programmes should be launched to deal with some priority elements.
4. For most of the Aq-SS systems of interest in the PA of repository systems, the solid radionuclide end-member is present in minor to trace amounts and, therefore, assuming its ideal solid solution behaviour is a reasonable first approximation.

5. There are a number of geochemical modelling codes that can handle solid solutions either in indirect (*i.e.*, PhreeqC, EQ3/6) or direct (*i.e.*, GEMS-PSI, ChemApp, HCh) way. Inverse modelling techniques like the dual-thermodynamic GEM approach have proven to be quite powerful to estimate end-member stoichiometries and to approximate non-ideal Aq-SS systems like the cement C-S-H phases with ideal solid solution models.

6. There are a number of well established macroscopic wet chemical methods which can be useful in determining some of macroscopic properties of Aq-SS systems. Calorimetric data is always very useful to close the appropriated thermodynamic cycles in Aq-SS. However, due to the atomistic nature of the solid solution incorporation, there is a need to complement macroscopic thermodynamic data with a detailed molecular characterisation. The current development of molecular simulation and atomic spectroscopic techniques will certainly bring more grounds under the determination of feasible Aq-SS models.

7. The applicability of Aq-SS thermodynamic models has already been explored for a number of systems of interest in the Performance Assessment of Nuclear Waste repositories, including the Ra(II)- Ba(II) sulphate system, the solubility of C-S-H phases, the uptake of trivalent lanthanides and actinides in calcite, and the dissolution behaviour of minor radionuclides present in solid solution in the UO_2 fuel matrix. In all cases, the combination of macroscopic chemical information with molecular spectroscopy methods has led development of chemically plausible Aq-SS thermodynamic models that agreed satisfactorily with the experimental observations.

Contents

PART I: Extended summary **1**

I.1 Introduction: scope, objectives and the audience of guidelines **1**

I.1.1 Motivation 1

I.1.2 Objectives 3

I.1.3 Audience 3

I.1.4 Scope 4

I.2 Definitions **4**

I.3 From Aqueous to Solid Solutions **7**

I.4 Basic thermodynamics of Solid Solutions **12**

I.4.1 The enthalpy of mixing 13

I.4.2 The entropy of mixing 13

I.4.3 Regular, subregular and generalised mixing models 14

I.4.4 Dilute solid solutions 14

I.4.5 On the relevance of non-ideality 14

I.4.6 Solid solution *versus* other uptake modes 16

I.4.7 Concepts and approximations in geochemical modelling of Aq-SS systems 17

I.4.7.1 Lippmann diagrams, a tool to visualise binary Aq-SS systems 18

I.4.8 Kinetic and thermodynamic approximations to Aq-SS in geochemical reactive transport modelling 18

I.5 Experimental and analytical aspects **19**

I.5.1 Synthesis procedures 20

I.5.2 Characterization of the solid solution 20

I.5.3 Solubility measurements in aqueous solutions 22

I.5.4 Partition/distribution experiments 22

I.5.5 Direct measurements of thermodynamic and mixing properties of solids in Aq-SS systems 23

I.5.5.1 Retrieval of excess Gibbs energy from electrochemical measurements 23

I.5.5.2 Calorimetry 23

I.6 Testing the Aq-SS concepts and methods in nuclear waste management relevant systems **25**

I.6.1 Radium and its incorporation into the barite solid solution family: environmental implications 25

I.6.1.1 The radium-barite relationship in natural and anthropogenic environments 25
I.6.1.2 Numerical modelling involving $(Ba,Ra)SO_4$ solid solutions 26
I.6.1.3 Conclusions 27
I.6.2 Cement phases – Solubility of calcium silicate hydrates (C-S-H) 27
I.6.2.1 Relevance of cement phases in radioactive waste management 27
I.6.2.2 Thermodynamic modelling of C-S-H and its limitations 27
I.6.2.3 Geochemical modelling of C-S-H systems of interest in radioactive waste management 28
I.6.2.4 Conclusions 29
I.6.3 Structural incorporation of trivalent actinides/lanthanides into Calcite 29
I.6.3.1 The relevance of calcite for radioactive waste management 29
I.6.3.2 Macroscopic information related to the sorption of f-elements into calcite 30
I.6.3.3 Spectroscopic information on the incorporation of f-elements into the calcite structure 30
I.6.3.4 Thermodynamic modelling of the Eu(III)/calcite system 31
I.6.3.5 Conclusions 31
I.6.4 Solid solutions in the nuclear fuel cycle 31
I.6.4.1 The applicability of Aq-SS thermodynamics to spent nuclear fuel 31
I.6.4.2 Main results from the characterisation of UO_2 spent nuclear fuel 32
I.6.4.3 Application of Aq-SS thermodynamics to spent fuel dissolution data 32
I.6.4.4 Conclusions 33
I.7 Report conclusions 33

PART II: Theory, experimental aspects and cases for study 35

II.1 Theoretical aspects of solid solutions and their solubility 35
II.1.1 Theory of solid solutions 35
II.1.1.1 Introduction 35
II.1.1.2 Thermodynamic formalism 37
II.1.1.3 The entropy of mixing 40
II.1.1.4 Regular, subregular and generalised mixing models 44
II.1.1.4.1 Dilute solid solutions 49
II.1.1.5 Phases with different structures 51
II.1.1.6 Order-disorder phenomena 55
II.1.1.6.1 General comments 55
II.1.1.6.2 An example: carbonates with calcite and dolomite structure 56
II.1.2 Methods and tools for thermodynamic description of aqueous-solid solution (Aq-SS) equilibria 60
II.1.2.1 Definitions and basic thermodynamics relations 62

II.1.2.1.1 Mole fraction scale 64
II.1.2.1.2 Molality scale 65
II.1.2.1.3 Aqueous activity coefficients 66
II.1.2.1.3.1 SIT Model 69
II.1.2.1.3.2 Pitzer Model 70
II.1.2.1.3.3 Extended UNIQUAC Model 70
II.1.2.1.3.4 Gas mixtures and gas solubility 71
II.1.2.1.3.5 Solid solubility 72
II.1.2.1.3.6 Unified theory of ionic solid solution solubilities 74
II.1.2.1.3.7 Multicomponent ionic Aq-SS system 76
II.1.2.2 Lippmann diagrams, a tool to visualise binary Aq-SS systems 77
II.1.2.2.1 Example of the use of Lippmann diagrams 80
II.1.2.3 Law of mass action (LMA) method for computing equilibrium speciation 86
II.1.2.4 Gibbs energy minimisation (GEM) method 94
II.1.2.4.1 GEM IPM algorithm 97
II.1.2.4.2 GEM dual-thermodynamic calculations in forward modelling 101
II.1.2.4.3 Multiple solid solutions and miscibility gaps 103
II.1.3 Methods of retrieval of stoichiometry, stability of solid solution end-members, and parameters of non-ideal mixing (inverse modeling) 105
II.1.3.1 The “activity ratios” technique 105
II.1.3.2 Dual Thermodynamic retrieval calculations 109
II.1.3.2.1 Algorithm of the single Dual-Th calculation at equilibrium 110
II.1.3.2.2 Retrieval of activity coefficients and mixing parameters 110
II.1.3.2.3 Retrieval of end-member standard Gibbs energy and solubility product at equilibrium 112
II.1.3.2.4 Retrieval of apparent molar Gibbs energy for a trace end-member 113
II.1.3.2.5 Dual-Th retrieval calculations at minimum stoichiometric saturation 113
II.1.3.2.6 Statistical Dual-Th calculations 115
II.1.3.2.7 Example: Eu^{III} in calcite 116
II.1.3.3 Graphical fitting and regression methods 120
II.1.3.3.1 Weighted least-squares and Bayesian estimation techniques 121
II.1.3.4 Retrieval of excess Gibbs energy from electrochemical measurements 122
II.1.3.5 Estimation of interaction parameters from the position of miscibility gaps 125
II.1.3.5.1 Miscibility gap data 126
II.1.3.5.2 Critical mixing point data 127
II.1.3.6 Estimation of interaction parameters from distribution coefficients 129

II.2 Experimental and analytical aspects 130
II.2.1 Co-precipitation experiments in aqueous solution 131
II.2.1.1 Limitations and points to notice 131
II.2.1.1.1 Synthesis procedures 134
II.2.2 Solubility measurements in aqueous solutions 136
II.2.2.1 Thermodynamic equilibrium solubility 137
II.2.2.2 Stoichiometric saturation 139
II.2.3 Solid phase characterisation 142
II.3 Cases of specific interest in relevant systems 155
II.3.1 Sulphates: the barite isostructural family and the incorporation of radioactive isotopes of Ra 155
II.3.1.1 Introduction to the barite isostructural family 155
II.3.1.2 The radium and its incorporation into the barite solid solution family: environmental implications 158
II.3.1.2.1 The radium-barium relationship in natural and anthropogenic environments 158
II.3.1.2.2 Numerical modelling involving (Ba,Ra)SO_4 solid solutions 160
II.3.1.3 Conclusions 168
II.3.2 Cases study/Cement phases – Solubility of calcium silicate hydrates (C-S-H) 169
II.3.3 Structural incorporation of trivalent actinides/lanthanides into Calcite 184
II.3.4 Solid solutions in the nuclear fuel cycle 193
II.3.4.1 Introduction 193
II.3.4.2 Solid solution in nuclear materials 194
II.3.4.2.1 Uraninite and non irradiated fuel 194
II.3.4.2.2 Irradiated UO_2 195
II.3.4.2.3 Mixed oxide (MOX) and Rock-like oxide (ROX) 196
II.3.4.3 Application of Aq-SS thermodynamics to spent fuel dissolution experimental data 196
II.3.4.3.1 Strontium 197
II.3.4.3.2 Barium 199
II.3.4.3.3 Neptunium 200
II.3.4.3.4 Plutonium 201
II.3.4.3.5 Lanthanides 202
II.3.4.4 Final remarks 203
Bibliography 205
List of cited authors 249

List of Figures

Figure I-1: Basic processes of absorbate molecules or atoms at mineral-water interface. 9

Figure I-2: Formation sequence of Zn/Mg phyllosilicate as monitored by EXAFS 11

Figure II-1: Schematic Gibbs energy of mixing curves for solid solutions 38

Figure II-2: Gibbs energy of mixing, solvus, and activity-composition relations for a regular solution with an interaction parameter of 16.6 kJ·mol^{-1} 46

Figure II-3: Gibbs energy of mixing for a system showing immiscibility at the temperature of interest 48

Figure II-4: Representation of solvus (binodal), spinodal, and coherent spinodal (taking interfacial energy or strain into account) in a binary system. 48

Figure II-5: Schematic representation of excess Gibbs energy in DQF for a binary solid solution AB showing a simple composition range where the regular mixing model is applicable 52

Figure II-6: Phase diagrams for the $CdCO_3$-$MgCO_3$ and $CaCO_3$-$MgCO_3$ systems 57

Figure II-7: Lippmann diagram of the $CoCO_3$-$MnCO_3$-H_2O system constructed using $K_{s,0}$ values from Table II 2, and subregular interaction parameters $A_0 = 3.61$ and $A_1 = -0.61$ 82

Figure II-8: Equilibrium *x*-*x* partition diagram for the same model as shown on Figure II-7 83

Figure II-9: Lippmann diagram of the $CaCO_3$-$SrCO_3$-H_2O system at 25 ºC constructed using $\log_{10} K_{s,0} = -8.34$ for aragonite, $\log_{10} K_{s,0} = -9.27$ for strontianite, and Redlich-Kister subregular interaction parameters $\alpha_0 = 3.43$ and $\alpha_1 = -1.82$ 84

Figure II-10: Equilibrium *x*-*x* (partition) diagram for the same system and model as shown on Figure II-9 84

Figure II-11: Lippmann diagram of the $SrSO_4$-$BaSO_4$-H_2O system at 25 ºC constructed using $\log_{10} K_{s,0} = -6.63$ for celestite, $\log_{10} K_{s,0} = -9.98$ for barite, binodal mole fractions of barite 0.021 and 0.979, and regular interaction parameter $\alpha_0 = 4.01$ ($\alpha_1 = 0$) determined from binodal compositions using the MBSSAS program 85

Figure II-12: The *x*-*x* (partition) diagram for the same system as shown on Figure II-11 86

Figure II-13: Flow chart of the "swap procedure" for finding an equilibrium assemblage of pure (stoichiometric) mineral phases in aquatic 89

Figure II-14: Flow chart of the extended LMA procedure for finding an equilibrium assemblage of pure mineral phases together with a solid solution or a gas mixture in the aquatic system. 93

Figure II-15: Simplified flow chart of the two-stage enhanced-precision GEM IPM algorithm 100

Figure II 16: Lippmann diagram plotted using data from Table II-4 and Table II-5 109

Figure II-17: Experimental results compared with predicted isotherms based on the same ternary $EuH(CO_3)_2$-$EuO(OH)$-$CaCO_3$ ideal solid solution model with g°_{298} values of −1773, −995, and −1129.2 kJ·mol^{-1}, respectively 120

Figure II-18: $G^E_m / x(1-x)$ *vs.* $x(MnCO_3)$ of the system $Co_{1-x}Mn_xCO_3$ 125

Figure II-19: Solid-solute phase diagram of Co-Mn carbonates at 323 K 126

Figure II-20: Lippmann diagram for the (Ba,Sr)SO_4-H_2O system: $\log_{10} K_{sp}(BaSO_4) = -9.97$; $\log_{10} K_{sp}(SrSO_4) = -6.63$ and $\alpha_0 = 2.0$ 137

Figure II-21: Congruent dissolution and primary saturation state, $\Sigma\Pi_{ps}$, in the (Ba,Sr)SO_4-H_2O system: $\log_{10} K_{sp}(BaSO_4) = -9.97$; $\log_{10} K_{sp}(SrSO_4) = -6.63$ and $\alpha_0 = 2.0$ 138

Figure II-22: Stoichiometric saturation curves in the system (Ba,Sr)SO_4-H_2O for $x_{Barite} = 0.1$, 0.3, 0.5, 0.7 and 0.9 140

Figure II-23: Minimum stoichiometric saturation curve in the system (Ba,Sr)SO_4-H_2O 141

Figure II-24: Geometry for gas flow-mixing (bubbling) drop-solution calorimetry in a high-temperature Calvet solution calorimeter 154

Figure II-25: (a) Lippmann diagram for an ideal (Ba,Sr)SO_4 solid solution at 25 ºC. (b) Equilibrium $x_{Ba,aq}$ - x_{BaSO_4} (Roozeboom) plot 157

Figure II-26: Plots showing the co-precipitation of radium with barite and their effects on the remaining oil-field brine in the model reported by [2004ZHU$_2$] 161

Figure II-27: Sketch of the example modelled to illustrate the effect of the radium co-precipitation with barite 162

Figure II-28: Effect of the Ba/Ra ratio on the radium concentration in solution 164

Figure II-29: Evolution of radium concentration through time along the flow direction (X) in the case 1 165

Figure II-30: Precipitation of $RaSO_4$ due to the inflow of a Ra-bearing effluent from the plant 166

Figure II-31: Extension of the Ra-rich plume after 10,000 years in the two cases simulated 167

Figure II-32: Evolution of radium concentration through time along the flow direction (X) in the case 2 168

Figure II-33: A. "Dimeric" tobermorite-like structural motive of C-S-H; B. More polymerised C-S-H structure with sorbed cations and tetrahedral aluminate ions; C. Additional $Ca(OH)_2$ layer in high-Ca C-S-H structure. 171

Figure II-34: Effect of changing C/S ratio in high-Ca ("Jennite") end-member of C-S-H(II) on the shape of Ca solubility curve of the ideal solid solution between "Tob" $5/6Ca(OH)_2{\cdot}SiO_2{\cdot}5/6H_2O$ and "Jen" $x Ca(OH)_2{\cdot}SiO_2{\cdot}H_2O$ where x = 10/6; 11/6; 12/6 and 15/6 175

Figure II-35: An example of impact of the normalisation factor nSi (applied simultaneously to all four end-member stoichiometries) onto the shape Aq-SS curves for calculated total solubility of Ca and Si in the C-S-H-H_2O system as function of the total C/S ratio 176

Figure II-36: Solubility profile (A) and solid phase speciation (B) of C-S-H *vs.* C/S ratios at 1 bar25 ºC modelled with GEMS-PSI code using two ideal solid solutions C-S-H(I) and C-S-H(II) with G^{o}_{m} (298.15 K) values of end-members from the rightmost column of Table II-11 178

Figure II-37: A. simulated impact of dilution on Ca solubility and C/S ratio in C-S-H(II) (portlandite is present only at high S/W ratios); B: simulated impact of CO_2 titration on Ca solubility, pH, and C/S ratio in C-S-H(II) (excess calcite phase is present throughout) 179

Figure II-38: Example of GEM model simulation of Zn-doped "cement" leaching at 1% Zn in CSH loading, using Zn-C-S-H(II) solid solution with hardystonite end-member 181

Figure II-39: GEM simulation runs of Zn-doped "cement" leaching at 1 bar 25 ºC, dependence of Zn_{aq} on Zn loading (*z* in %, numbers at the curves 182

Figure II-40: Strontium concentrations determined in the leaching solution *vs.* strontium concentrations calculated assuming a congruent co-dissolution process 198

Figure II-41: Strontium *vs.* uranium concentrations in all the tests with the exception of those reaching a steady-state for ^{90}Sr 199

Figure II-42: Barium concentrations calculated assuming a congruent co-dissolution process with uranium *vs.* the ones determined in the leaching solution 200

Figure II-43: Neptunium *vs.* uranium concentrations in all the experimental series 201

Figure II-44: Comparison between the kinetic model and the experimental data 202

Figure II-45: Calculated concentrations *vs.* the experimental ones assuming a congruent co-dissolution process of the minor lanthanides 203

List of Tables

Table I-1: Overview of some selected analytical techniques to obtain key information of solid solution phases 21

Table II-1: Charge-coupled substitutions in minerals. 36

Table II-2: Solubility products of spherocobaltite $CoCO_3$ and rhodochrosite $MnCO_3$ at 50 ºC. 81

Table II-3: Experimental data on Aq-SS partitioning of K(Cl,Br) at 25 ºC 107

Table II-4: Calculations using Eqs. (II.199), (II.200) and data from Table II-3. 108

Table II-5: Regular Margules parameter WG ($kJ \cdot mol^{-1}$) found from the last column of Table II-4. 108

Table II-6: Final Eu molalities (m_{Eu}) and calculated Eu cationic mole fractions (χ_{Eu}) in calcite overgrowths precipitated at $p_{CO_2} \approx 1$ bar and 25 ºC, together with dual chemical potentials 117

Table II 7: Apparent molar Gibbs energies (g^{*}_{298}) estimated for seven Eu end-member candidates using Eq. (II.209) from dual elemental chemical potentials given in Table II-6. 118

Table II-8: Mean end-member standard Gibbs energies of formation g^{o}_{298} ($kJ \cdot mol^{-1}$) derived from DualTh calculations for the three considered datasets 119

Table II-9: Measured ΔE values and calculated G^{E}_{m} values for the $Co_{1-x}Mn_xCO_3$ solid solutions 124

Table II-10: Initial composition of the clay porewater and of the radium-bearing effluent. Concentrations are in $mol \cdot kg^{-1}$ water 163

Table II-11: Optimised C-S-H solid solutions model 177